Journal of Telecommunication, Electronic and Computer Engineering
ISSN: 2180 – 1843 e-ISSN: 2289-8131 Vol. 16 No. 2
jtec.utem.edu.my
DOI: https://doi.org/10.54554/jtec.2024.16.02.005

Frequency Octupling Radio over Fiber System with Multiple Remote Antenna Units

A. H. Hussein[1], S. Yaakob[1], S. B. A. Anas[1], Rawa Muayad Mahmood[1], Muhammad Zamzuri Abdul Kadir[2] and Azwan Mahmud[3]
[1]*WIPNET, Department of Computer and Communication Systems Engineering, Faculty of Engineering, Universiti Putra Malaysia (UPM), Serdang, Selangor, Malaysia.*
[2]*Kulliyyah of Science, International Islamic University Malaysia, Jalan Sultan Ahmad Shah, Bandar Indera Mahkota 25200, Kuantan, Pahang, Malaysia.*
[3]*Faculty of Engineering, Multimedia University, Cyberjaya 43650, Selangor, Malaysia.*
syamsuri@upm.edu.my

Article Info

Article history:
Received Mar 1st, 2024
Revised May 20th, 2024
Accepted June 28th, 2024
Published June 30th, 2024

Index Terms:
Millimeter wave
Radio over Fiber
Frequency Octupling
Remote Antenna Unit
Wavelength Reuse

Abstract

Bidirectional radio over fiber (RoF) transmission to multiple remote antenna units (RAUs) with frequency octupling is proposed in this paper. The proposed RoF system uses a dual-port Mach-Zehnder modulator (DP-MZM) and an arrayed waveguide grating (AWG) to generate millimeter-wave (mm-wave) to four different RAUs. Bit Error Rate (BER) and received optical power are key parameters used to measure the performance of the system. From the simulation results, it is shown that the proposed system achieves an acceptable performance a fiber distance of 50 km with a BER of 10^{-12}. Furthermore, the results indicate that the dispersion-induced power penalties for both uplink and downlink transmission of all RAUs are less than 1 dB. In summary, the proposed system simplifies the RoF system by reusing wavelengths and utilizing low RoF frequency through the frequency-octupling technique.

I. INTRODUCTION

With the rapid development of ultra-high-speed browsing, online mobile games, and high-definition videos, the need for high bandwidth wireless transmission has increased. While wired networks based on passive optical networks (PON) offer high bandwidth with low latency, they lack flexibility. In contrast, wireless networks provide flexibility to end users but are limited in their ability to deliver high bandwidth. Therefore, Radio over Fiber (RoF) technology, which integrates both wireless and wired communication is a viable solution [1][2]. RoF technology is becoming increasingly important due to its huge transmission capacity, transparency to bandwidth or modulation format, ability to support small remote stations (RSs), and possibilities for centralized operation [3].

The increasing demand for wireless communication network bandwidth is pushing the frequencies of the radio frequency (RF) carrier towards the millimeter-wave (mm-wave) bands. Compared to lower frequency carriers, mm-wave frequency bands have shorter transmission distances due to their high frequency range and are more susceptible to atmospheric effects and rain attenuation [4]. To accommodate the reduced transmission distance of mm-wave, the number of remote antenna units (RAU) must be increased and positioned closer to customer units. However, to make such networks practical, the RAU and the central station (CS) must be simple and efficient [4]-[7]. Omitting the RAU components and placing them at the common CS makes the RoF system smaller and simpler, leading to lower installation and operation costs [8].

Recent studies on the unlicensed 60 GHz mm-wave frequency have shown that it can deliver high data rates and support the increasing capacity demands [9][10]. However, electrical components, such as mixers and RF carrier generators are costly at 60 GHz frequency. In addition, as the RF frequency increases, the fiber-link distance is significantly limited due to the pronounced effect of dispersion [11]. A high frequency multiplication factor for the mm-wave generation technique eliminates the need for an RF local oscillator (LO) with a high frequency at the CS [12]. As a result, it is essential to increase the multiplication factor without increasing system complexity.

Several methods have been proposed to eliminate the need for a laser source and high-frequency LO at the RAU. A study in [13] proposed an RoF system for high-speed train communication by transmitting mm-wave signals to 10 different RAUs simultaneously. However, a separate laser source is required for the downlink transmission to each RAU. The work in [1] proposed a frequency-quadrupling based full-duplex RoF system. This system supports one RAU, and due to wavelength reuse, the carrier is reused for uplink data transmission at the RAU. Authors in [14] implemented a simple and cost effective full-duplex RoF system. They employed an optical interleaver and external modulator to produce mm-waves with frequency-octupling

that carry two orthogonal frequency-division multiplexing (OFDM) downlink data streams for two base stations (BS) and the wavelength-reuse for uplink connection. By using two-stage cascaded Mach-Zehnder modulators (MZM) with a parallel configuration, [12] demonstrated dual 16-tupling frequency generation that avoids the requirement for a high frequency LO at the CS and supports two BSs simultaneously. It is worth mentioning that, so far, all these proposed RoF systems only support two RAUs or less.

The authors in [15] proposed an RoF transmission system based on a multi-wavelength optical comb and pulse shaping with simultaneous wireless multimode operation using single optical carrier. In this arrangement, wireless carriers at 5 GHz, 25 GHz, 45 GHz, and 65 GHz have been obtained using direct detection. For the uplink transmission, there are three pure optical sources that can be used for uplink transmission. Moreover, a duplex RoF distributed antenna system (DAS) architecture based on polarization multiplexing was proposed by [16] to transmit data from the CS to 4 RAUs in a ring topology. [17] also proposed the transmission of two subcarrier multiplexed (SCM) mm-wave signals to four RAUs, with each RAU receiving 512 Mbps downlink data from the CS and transmitting 128 Mbps uplink data. However, the frequency multiplication factor is small, and a high frequency RF LO is required at the CS.

Minimizing the high-frequency RF LO at the CS can decrease the overall RoF system cost. Various multiplication techniques with different multiplication factors have been proposed, such as frequency doubling [18], tripling [19], quadrupling [1][20], sextupling [11][21], octupling [14][22][23], 12-tupling [24], and 16-tupling [12][25][26].

This paper proposes a bi-directional RoF system with multiple RAUs using a single laser source with frequency octupling. The CS uses a single laser source to serve four different RAUs simultaneously. This eliminates the need for a high-frequency RF LO at the CS, and the wavelength is reused for uplink data transmission, reducing the complexity of the system.

II. PRINCIPLE

Figure 1 shows the proposed RoF system architecture. The optical carriers are generated at the CS, which consists of a continuous wave (CW) laser source, dual port Mach-Zehnder modulator (DP-MZM), RF source, optical bandpass filter (OBPF), and arrayed waveguide grating (AWG).

The CW laser source generates a light wave with angular frequency ω_o.. The field of the light wave can be stated as: $\boldsymbol{E_o(t) = A_o e^{j\omega_o t}}$, where $\boldsymbol{A_o}$ is the amplitude of the Lightwave. The light wave is modulated using DP-MZM, driven by two RF sinusoidal, $\boldsymbol{V_1(t) = V_{LO}\cos\omega_{LO}t}$ and $\boldsymbol{V_2(t) = V_{LO}\cos(\omega_{LO}t + \theta)}$, where $\boldsymbol{V_{LO}}$, and $\boldsymbol{\omega_{LO}}$ are the amplitude voltage and angular frequency of the LO.

According to [20], the DP-MZM output can be written as:

$$E_{out} = \frac{E_c(t)}{10^{\alpha/20}}\left\{\gamma.\exp\left[j\pi\frac{v_{2(t)}}{v_\pi} + j\pi\frac{v_{b2}}{v_\pi}\right] + (1-\gamma).\exp\left[j\pi\frac{v_{1(t)}}{v_\pi} + j\pi\frac{v_{b1}}{v_\pi}\right]\right\} \quad (1)$$

The insertion loss of the DPMZM is α. $\boldsymbol{V_{b1}}$, $\boldsymbol{V_{b2}}$ and $\boldsymbol{\gamma}$ are the bias voltage 1, bias voltage 2 and the splitting ratio of the DP-MZM's two arms, respectively. For optimal performance, it is assumed that $\boldsymbol{\alpha} = 0$ and $\boldsymbol{\gamma}$ is 0.5. Therefore, the optical spectrum components depend on $\boldsymbol{V_{b1}}$, $\boldsymbol{V_{b2}}$, and $\boldsymbol{\theta}$, which can be adjusted to obtain different optical mm-waves spectra. From equation 1, the output light wave can be written as:

$$E_{out} = \frac{E_c}{2}\left\{\cos[\omega_o t + \frac{\pi V_{LO}}{V_\pi}cos(\omega_{LO}t + \theta) + \frac{\pi V_{b2}}{V_\pi}] + \cos[\omega_o t + \frac{\pi V_{LO}}{V_\pi}\cos(\omega_{LO}t) + \frac{\pi V_{b1}}{V_\pi}]\right\} \quad (2)$$

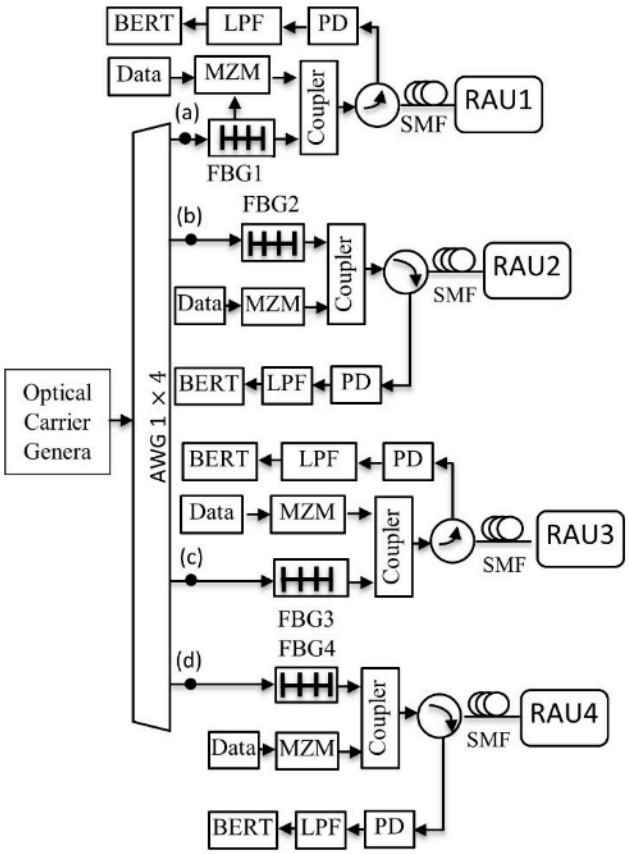

(a)

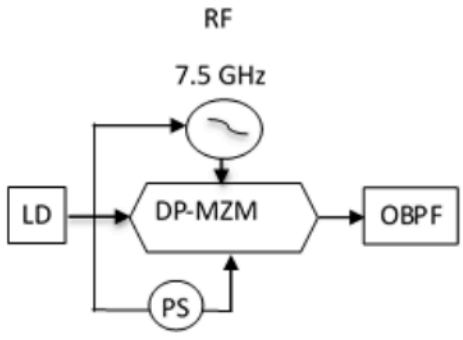

(b)

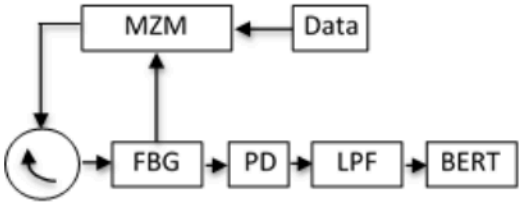

(c)

Figure 1. (a) Proposed RoF System Block Diagram (b) Carrier Generation Block Diagram (c) RAU Block Diagram

By taking $m = \frac{\pi V_{LO}}{V_\pi}$ which is phase modulation index,

$\varphi_1 = \frac{\pi V_{b1}}{V_\pi}$ and $\varphi_2 = \frac{\pi V_{b2}}{V_\pi}$, the equation can be simplified as:

$$E_{out} = \frac{E_c}{2}\{\cos[\omega_o t + m\cos(\omega_{LO}t + \theta) + \varphi_2] + \cos[\omega_o t + m\cos(\omega_{LO}t) + \varphi_1]\} \quad (3)$$

The equation can be expanded using Bessel function as following:

$$E_{out} = \frac{E_c}{2}\{\cos(\omega_o t + \varphi_2)[j_O(m) + 2\sum_{n=1}^{\infty}(-1)^n J_{2n}(m)[\cos(2n\omega_{LO}t)\cos(2n\theta) - \sin(2n\omega_{LO}t)\sin 2n\theta]] + 2\sin(\omega_o t + \varphi_2)\sum_{n=1}^{\infty}(-1)^n J_{2n-1}(m)[\cos[(2n-1)\omega_{LO}t]\cos[(2n-1)\theta] - \sin[(2n-1)\omega_{LO}t]\sin[(2n-1)\theta] + \cos(\omega_o t + \varphi_1)[j_O(m) + 2\sum_{n=1}^{\infty}(-1)^n J_{2n}(m)[\cos(2n\omega_{LO}t)] + 2\sin(\omega_o t + \varphi_1)\sum_{n=1}^{\infty}(-1)^n J_{2n-1}(m)[\cos((2n-1)\omega_{LO}t)]\} \quad (4)$$

where Jn(m) is the nth order Bessel function of the first kind. We take $= \pi$, $V_{b1} = 0$, and $V_{b2} = V_\pi$, the equation can be simplified as:

$$E_{out} = 2E_C \sin\omega_o t \sum_{n=1}^{\infty}(-1)^n J_{2n-1}(m)[\cos((2n-1)\omega_{LO}t) \quad (5)$$

By biasing the DP-MZM at null point, the carrier and the even indexed sidebands can be eliminated. High order sidebands, which are higher than the 11th order is eliminated because of their low magnitude. Therefore, we get:

$$\begin{aligned} E_{out} = {} & -2E_C J_1[(m)\sin(\omega_o t + \omega_{LO}t) + \sin(\omega_o t - \omega_{LO}t)] + \\ & 2E_C J_3[(m)\sin(\omega_o t + 3\omega_{LO}t) + \sin(\omega_o t - 3\omega_{LO}t)] - 2E_C J_5[(m) \\ & \sin(\omega_o t + 5\omega_{LO}t) + \sin(\omega_o t - 5\omega_{LO}t)] + \\ & 2E_C J_7[(m)\sin(\omega_o t + 7\omega_{LO}t) + \\ & \sin(\omega_o t - 7\omega_{LO}t)] - 2E_C J_9[(m) \\ & \sin(\omega_o t + 9\omega_{LO}t) + \sin(\omega_o t - 9\omega_{LO}t)] + \\ & 2E_C J_{11}[(m)\sin(\omega_o t + 11\omega_{LO}t) + \\ & \sin(\omega_o t - 11\omega_{LO}t)] \end{aligned} \quad (6)$$

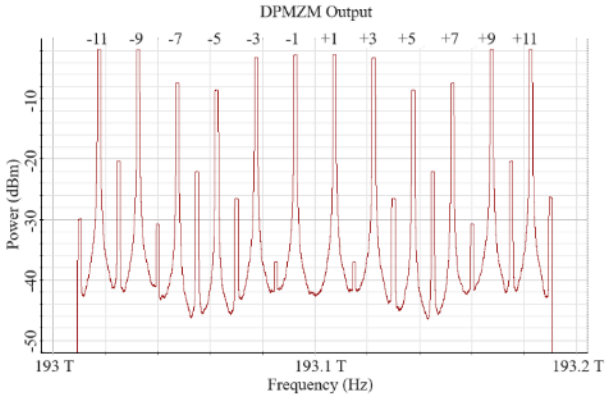

Figure 2. Optical Spectrum of DP-MZM Output

After passing the signal into 1×4 AWG, it is divided into four parts as shown in Figure 3.

$$E_{out1} = 2E_C J_{11}(m)\sin(\omega_o t - 11\omega_{LO}t) + 2E_C J_3(m)\sin(\omega_o t - 3\omega_{LO}t) - 2E_C J_5(m)\sin(\omega_o t + 5\omega_{LO}t) \quad (7)$$

$$E_{out2} = -2E_C J_5(m)\sin(\omega_o t - 5\omega_{LO}t) + 2E_C J_3(m)\sin(\omega_o t + 3\omega_{LO}t) + 2E_C J_{11}(m)\sin(\omega_o t + 11\omega_{LO}t)$$

$$E_{out3} = 2E_C J_7(m)\sin(\omega_o t - 7\omega_{LO}t) - 2E_C J_1(m)\sin(\omega_o t + \omega_{LO}t) - 2E_C J_9(m)\sin(\omega_o t + 9\omega_{LO}t)$$

$$E_{out4} = -2E_C J_9(m)\sin(\omega_o t - 9\omega_{LO}t) - 2E_C J_1(m)\sin(\omega_o t - \omega_{LO}t) + 2E_C J_7(m)\sin(\omega_o t + 7\omega_{LO}t)$$

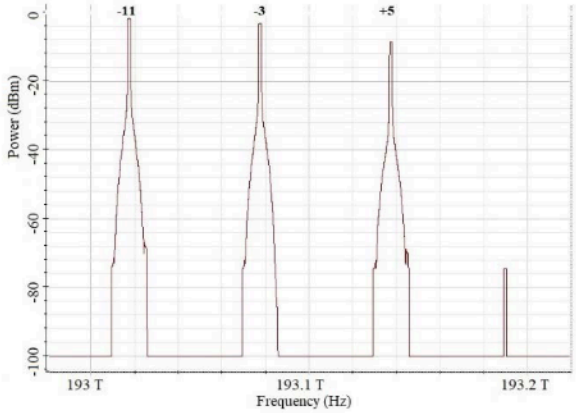

(a)

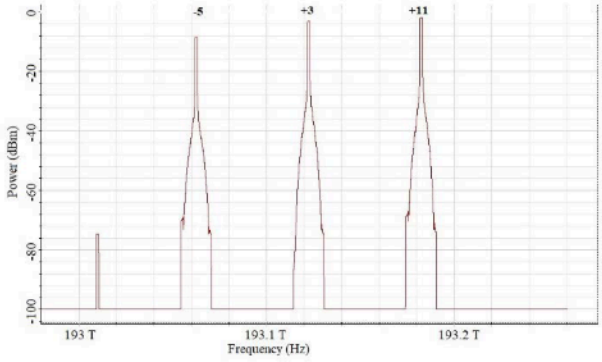

(b)

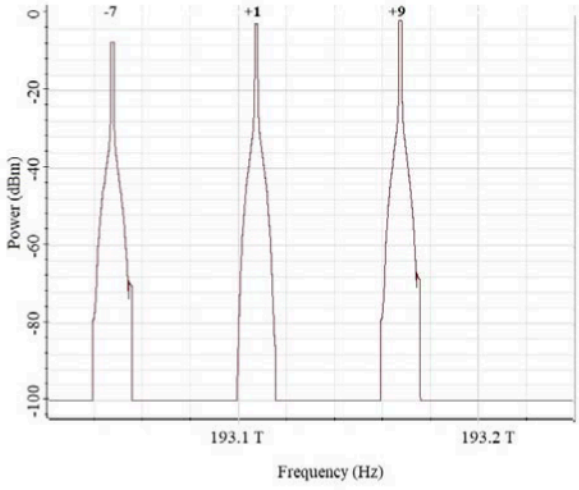

(c)

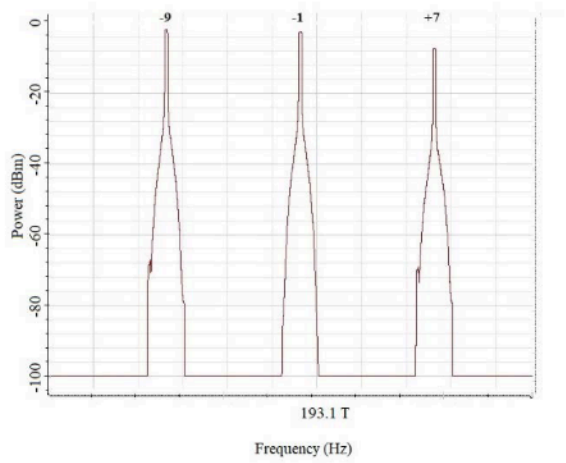

(d)

Figure 3. The optical spectra at points a, b, c, and d labeled in Figure 1.

III. SIMULATION SETUP

The simulated setup used to verify the proposed system is illustrated in Figure 1. The performance of the system is evaluated for both uplink and downlink transmission using OptiSystem 17.1. A CW laser source with 0 dBm optical power, a 10 MHz linewidth, and a central frequency of 193.1 THz is modulated, via a DP-MZM, driven by a 7.5 GHz RF sinusoidal clock. The 7.5 GHz frequency was chosen because electrical components like mixers and RF carrier generators become significantly more expensive at higher frequencies, such as 60 GHz. By employing frequency octupling, we can achieve the desired 60 GHz output while leveraging the cost-effectiveness of lower frequency components. The switching RF voltage and bias voltages are both set to 4 V in the simulation. The modulation voltage V_{LO}, V_{b1} and V_{b2} are set to 15V, 0V and 4V, respectively. An OBPF is used at the DP-MZM output to eliminate unwanted high-order sidebands. The optical spectrum of OBPF output is shown in Figure 2. The output of the OBPF is fed to 1×4 AWG with a starting frequency of 193.0175 THz and a channel spacing of 15 GHz. The AWG divides the carrier into four different channels, each containing three sidebands. For RAU1, $(\omega_o - 3\omega_{LO})$ is reflected by fiber Bragg grating (FBG) 1 and is modulated by MZM 1, which is driven by a 5 Gb/s Pseudo-Random Bit Sequence (PRBS). Then the modulated signal and unmodulated sidebands, $(\omega_o - 11\omega_{LO})$ and $(\omega_o + 5\omega_{LO})$ are combined and sent to RAU 1 through a 50 km bidirectional single-mode fiber (SMF). At RAU1, $(\omega_o + 5\omega_{LO})$ reflected by FBG2, is modulated by MZM2 driven by 5 Gb/s PRBS uplink data and sent back to the CS. The negative eleventh order sideband $(\omega_o - 11\omega_{LO})$ and the negative third order sideband $(\omega_o - 3\omega_{LO})$ are detected by a photodetector (PD) with 0.9 responsivity and then converted into a 60 GHz electrical mm-wave. Figure 4 shows the RF signal of RAU 1 after passing through the PIN photodetector in the frequency domain. The uplink data sent to the CS is detected using a PIN photodetector and then passed to a low pass filter (LPF). A variable attenuator is utilized before the photodetector to control the received optical power and measure the uplink and downlink transmission performance. All the other RAUs have similar architectures to that of RAU1.

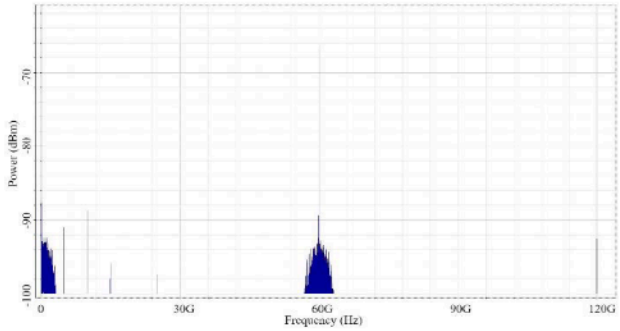

Figure 4. RF Signal in Frequency Domain for RAU 1

For RAU2, $(\omega_o + 3\omega_{LO})$ is used to modulate the downlink data and is then combined with $(\omega_o - 5\omega_{LO})$ and $(\omega_o + 11\omega_{LO})$. The negative fifth order sideband $(\omega_o - 5\omega_{LO})$ is reflected by FBG4 at RAU2 and is used to modulate the uplink data from RAU2, which is then sent back to the CS. $(\omega_o + 3\omega_{LO})$ and $(\omega_o + 11\omega_{LO})$ are detected by PD to generate electrical mm-wave. For RAU3, $(\omega_o + \omega_{LO})$ is used to modulate the downlink data and is then combined with $(\omega_o - 7\omega_{LO})$ and $(\omega_o + 9\omega_{LO})$ sidebands. $(\omega_o - 7\omega_{LO})$ is reflected by FBG6 at RAU3 and then is used to modulate the uplink data from RAU3 to the CS. The sidebands $(\omega_o + 9\omega_{LO})$ and $(\omega_o + \omega_{LO})$ are detected by PD to generate electrical mm-wave. Lastly, $(\omega_o - \omega_{LO})$ is used to modulate the downlink data from the CS to RAU4. FBG8 is used to reflect the uplink carrier $(\omega_o + 7\omega_{LO})$. The sidebands $(\omega_o - \omega_{LO})$ and $(\omega_o - 9\omega_{LO})$ are detected by PD to generate electrical mm-wave. Parameter values used for the proposed system are shown in Table 1.

Table 1
Simulation parameters of the proposed system

Parameter	Value
Laser power	10 dBm
Linewidth of LD	10 MHz
Laser frequency	193.1 THz
Length of SMF	50 km
Dispersion	16.75 ps/nm/km
Dispersion Slope	0.075 ps/nm2/km
Attenuation coefficient	0.2 dB/km
Switching Bias voltage	4 V
Switching RF voltage	4 V
Bias Voltage 1	0 V
Bias Voltage 2	4 V
RF Frequency	7.5 GHz

IV. RESULTS AND DISCUSSIONS

In this section, the simulation results of the proposed RoF system for both uplink and downlink signals are presented. To evaluate the performance of each RAU, the BER of back-to-back (B-T-B) and 50km transmission is investigated. To vary the power of the received signal, an optical attenuator (OA) is used right before the photodetector, and the differences in the BER results are achieved by varying the received optical power (ROP). The corresponding values of the BER versus ROP are shown in Figure 5. For high-speed optical communication systems, the required BER is now in the range of 10^{-9} to 10^{-15}, with a typical value of 10^{-12}[1]. In this simulation, the specified BER is 10^{-12}.

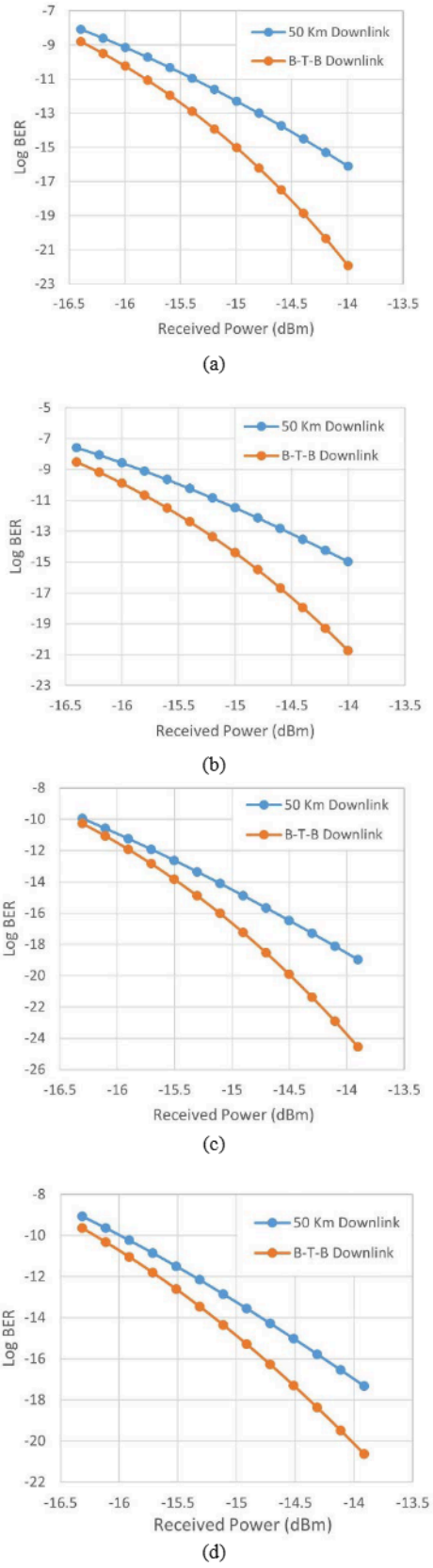

Figure 5. BER vs ROP for B-T-B and 50 km Downlink Transmission (a) RAU 1 (b) RAU 2 (c) RAU 3 (d) RAU 4.

We can see that the dispersion-induced power penalty at 10^{-12} BER is less than 1 dB for all RAUs after 50km transmission. The power penalty of the downlink transmission for RAU1, RAU2, RAU3, and RAU4 at BER 10^{-12} are 0.6 dB,0.6 dB,0.4 dB, and 0.4 dB, respectively. The differences in power penalties among the RAUs can be attributed to the varying power levels of the sidebands used for downlink data modulation.

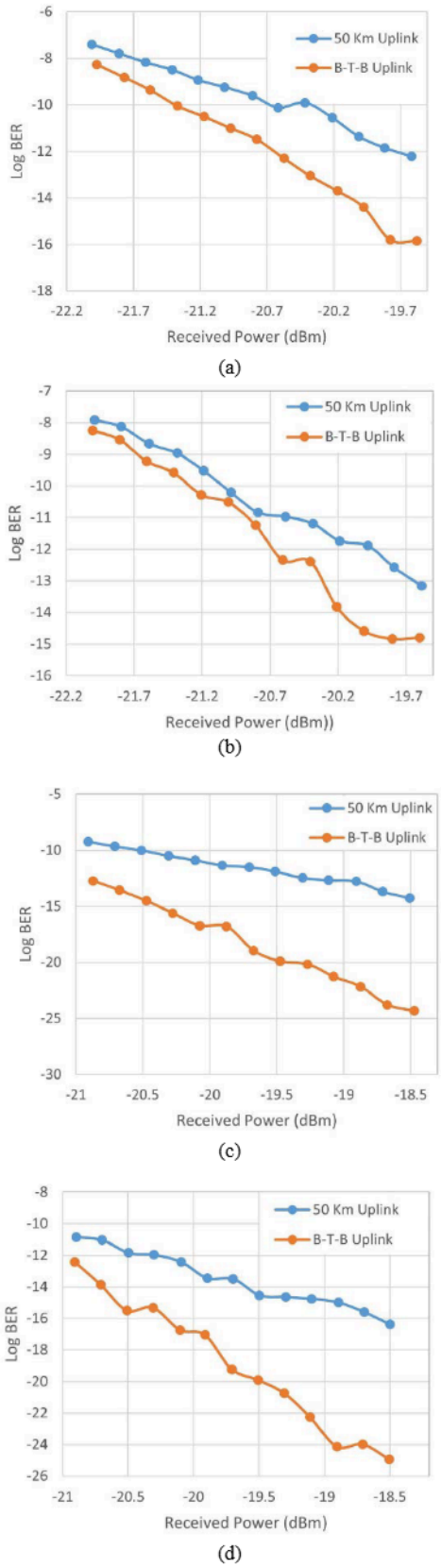

Figure 6. BER vs ROP for B-T-B and 50 km uplink Transmission (a) RAU 1 (b) RAU 2 (c) RAU 3 (d) RAU 4.

For the uplink, as shown in Figure 6, the power penalties for RAU1, RAU2, RAU3 and RAU4 are 0.6 dB, 0.3 dB, 0.4 dB, and 0.5 dB respectively, at BER 10^{-12}. The BER curves

shift slightly to the right compared to the B-T-B transmission. This shift represents a dispersion-induced power penalty due to the extended fiber length. However, this penalty remains below 1 dB for all RAUs, showcasing the system's resilience to signal degradation over longer distances.

The use of a single laser source and frequency octupling technique minimizes the complexity and cost of the system by supporting multiple RAUs simultaneously without significant signal degradation.

V. CONCLUSION

This paper proposes a simple bi-directional RoF transmission system that supports 4 RAUS simultaneously using a single laser source. The simulation results show that the power penalty for both downlink and uplink transmission is less than 1 dB for all four RAUs, indicating good performance of the proposed system. In this system, no additional laser source is required at the RAU due to the use of wavelength reuse, and the LO frequency is significantly reduced using the frequency octupling technique.

ACKNOWLEDGEMENT

This work supported by the Fundamental Research Grant (FRGS), Ministry of Higher Education, Malaysia, No. FRGS/1/2019/TK04/UPM/02/07 and Inisiatif Putra Muda Grant by Universiti Putra Malaysia, No. GP-IPM/2017/9524100.

REFERENCES

[1] Y. He et al., "A full-duplex 100-GHz radio-over-fiber communication system based on frequency quadrupling," Optik, vol. 175, pp. 148-153, 2018/12/01/ 2018.

[2] R. S. Asha, V. K. Jayasree, and S. Mhatli, "An 80Gbps multi-band access radio over fiber link with single side band optical millimeter-wave dispersion-tolerant transmission without FBG and optical filter," Opto-Electronics Review, vol. 25, no. 4, 2017, pp. 311-317.

[3] S. Yaakob et al., "Minimal optimization technique for radio over fiber WLAN transmission in IM-DD optical link," vol. 52, no. 4, 2010, pp. 812-815.

[4] M. A. Hameed and R. Hui, "Simplified RF Carrier Extraction and Reuse in OFDM Radio-Over-Fiber Systems," IEEE Photonics Technology Letters, vol. 26, no. 17, 2014, pp. 1734-1737.

[5] W. Xu, X. Gao, M. Zhao, M. Xie, and S. Huang, "Full duplex radio over fiber system with frequency quadrupled millimeter-wave signal generation based on polarization multiplexing," Optics & Laser Technology, vol. 103, 2018, pp. 267-271.

[6] A. Liu, H. Yin, and B. Wu, "High-efficient full-duplex WDM-RoF system with sub-central station," Optics Communications, vol. 414, 2018, pp. 72-76.

[7] V. A. Thomas, M. El-Hajjar, and L. Hanzo, "Millimeter-Wave Radio Over Fiber Optical Upconversion Techniques Relying on Link Nonlinearity," IEEE Communications Surveys & Tutorials, vol. 18, no. 1, 2016, pp. 29-53.

[8] S. Yaakob, M. Z. A. Kadir, S. M. Idrus, N. M. Samsuri, R. Mohamad, and N. E. J. O. Farid, "On the carrier generation and HD signal transmission using the millimeter-wave radio over fiber system," vol. 124, no. 23, 2013, pp. 6172-6177.

[9] R. Al-Dabbagh and H. Al-Raweshidy, "64-GHz millimeter-wave photonic generation with a feasible radio over fiber system," vol. 56 %J Optical Engineering, no. 2, p. 026117, 2017.

[10] D. Novak et al., "Radio-Over-Fiber Technologies for Emerging Wireless Systems," IEEE Journal of Quantum Electronics, vol. 52, no. 1, pp. 1-11, 2016.

[11] K. Yang, X. G. Huang, J. H. Zhu, and W. J. Fang, "Transmission of 60 GHz wired/wireless based on full-duplex radio-over-fibre using dual-sextupling frequency," IET Communications, vol. 6, no. 17, pp. 2900-2906, 2012.

[12] K. E. Muthu and A. S. J. J. o. t. E. O. S.-R. P. Raja, "Bidirectional MM-Wave Radio over Fiber transmission through frequency dual 16-tupling of RF local oscillator," vol. 12, no. 1, pp. 1-9, 2016.

[13] A. Kanno, P. T. Dat, N. Yamamoto, and T. Kawanishi, "Millimeter-wave radio-over-fiber system for high-speed railway communication," in 2016 Progress in Electromagnetic Research Symposium (PIERS), 2016, pp. 3911-3915.

[14] J. S. B. Joseph Zacharias, Vijayakumar Narayanan, "82 GHz Millimeter-Wave Transmission Over OFDM ROF System," International Journal of Engineering and Advanced Technology (IJEAT), vol. 6, no. 1, 2016.

[15] G. Li, Z. Lin, X. Huang, and J. J. E. Li, "A radio over fiber system with simultaneous wireless multi-mode operation based on a multi-wavelength optical comb and pulse-shaped 4QAM-OFDM," electronics, vol. 8, no. 10, p. 1064, 2019.

[16] T. Mehmood, H. Qayyum, and S. Ghafoor, "Polarization multiplexing based duplex radio-over-fiber link for millimeter wave signal transmission to a ring of multiple radio access units," Frontiers of Information Technology & Electronic Engineering, vol. 20, no. 2, pp. 300-306, 2019/02/01 2019.

[17] T. Mehmood and S. Ghafoor, "Millimeter-wave signal generation and transmission to multiple radio access units by employing nonlinearity of the optical link," International Journal of Communication Systems, https://doi.org/10.1002/dac.3830 vol. 32, no. 1, p. e3830, 2019/01/10 2019.

[18] W. Xu et al., "High spectral purity millimeter wave generation and wavelength reuse radio over fiber system based on modified double sideband," in 2016 25th Wireless and Optical Communication Conference (WOCC), 2016, pp. 1-4: IEEE.

[19] Q. Wang, H. Rideout, F. Zeng, and J. J. I. P. T. L. Yao, "Millimeter-wave frequency tripling based on four-wave mixing in a semiconductor optical amplifier," vol. 18, no. 23, pp. 2460-2462, 2006.

[20] J. H. Zhu, X. G. Huang, and J. L. Xie, "A full-duplex radio-over-fiber system based on dual quadrupling-frequency," Optics Communications, vol. 284, no. 3, pp. 729-734, 2011/02/01/ 2011.

[21] K. E. Muthu and A. S. Raja, "Frequency sextupling using single LN-MZM and 2.5 Gb/s RoF transmission," in 2016 International Conference on Wireless Communications, Signal Processing and Networking (WiSPNET), 2016, pp. 1842-1844: IEEE.

[22] G. Cheng, B. Guo, S. Liu, and W. J. O. Fang, "A novel full-duplex radio-over-fiber system based on dual octupling-frequency for 82 GHz W-band radio frequency and wavelength reuse for uplink connection," vol. 125, no. 15, pp. 4072-4076, 2014.

[23] A. B. Dar, F. J. O. Ahmad, and Q. Electronics, "A full-duplex 40 GHz radio-over-fiber transmission system based on frequency octupling," vol. 51, no. 10, pp. 1-11, 2019.

[24] Z. Zhu, S. Zhao, Y. Li, X. Chu, X. Wang, and G. J. I. J. o. Q. E. Zhao, "A radio-over-fiber system with frequency 12-tupling optical millimeter-wave generation to overcome chromatic dispersion," vol. 49, no. 11, pp. 919-922, 2013.

[25] G. J. O. Shanmugapriya, "Frequency16-tupled optical millimeter wave generation using dual cascaded MZMs and 2.5 Gbps RoF transmission," vol. 140, pp. 338-346, 2017.

[26] S. Liu and J. Ma, "Filterless frequency 16-tupling millimeter-wave signal generation with cascaded Mach–Zehnder modulators," vol. 60, no. 1, Optical Engineering, 2021, https://doi.org/10.1117/1.OE.60.1.015101.